Journal of Power Sources 195 (2010) 6805–6810

Contents lists available at ScienceDirect

Journal of Power Sources

journal homepage: www.elsevier.com/locate/jpowsour

Influence of conductive additives and surface fluorination on the charge/discharge behavior of lithium titanate ($Li_{4/3}Ti_{5/3}O_4$)

Hidetoshi Utsunomiya [a], Tsuyoshi Nakajima [a,*], Yoshimi Ohzawa [a], Zoran Mazej [b], Boris Žemva [b], Morinobu Endo [c]

[a] Department of Applied Chemistry, Aichi Institute of Technology, Yakusa, Toyota 470-0392, Japan
[b] Jožef Stefan Institute, Ljubljana 1000, Slovenia
[c] Department of Electrical and Electronic Engineering, Shinshu University, Nagano 380-8553, Japan

ARTICLE INFO

Article history:
Received 2 April 2010
Received in revised form 26 April 2010
Accepted 26 April 2010
Available online 20 May 2010

Keywords:
Lithium titanate
Conductive additive
Surface fluorination
Lithium ion battery

ABSTRACT

Effect of conductive additives and surface modification with NF_3 and ClF_3 on the charge/discharge behavior of $Li_{4/3}Ti_{5/3}O_4$ (≈4.6 μm) was investigated using vapor grown carbon fiber (VGCF) and acetylene black (AB). VGCF and mixtures of VGCF and AB increased charge capacities of original $Li_{4/3}Ti_{5/3}O_4$ and those fluorinated with NF_3 by improving the electric contact between $Li_{4/3}Ti_{5/3}O_4$ particles and nickel current collector. Surface fluorination increased meso-pore with diameter of 2 nm and surface area of $Li_{4/3}Ti_{5/3}O_4$, which led to the increase in first charge capacities of $Li_{4/3}Ti_{5/3}O_4$ samples fluorinated by NF_3 at high current densities of 300 and 600 mA g^{-1}. The result shows that NF_3 is the better fluorinating agent for $Li_{4/3}Ti_{5/3}O_4$ than ClF_3.

1. Introduction

Recent research interest for lithium ion batteries is the development of high power electric sources for hybrid cars and electric vehicles. New electrode materials with high rate charge/discharge are urgently required for this purpose. It was reported that electrochemical intercalation and deintercalation of lithium ion is reversible in lithium titanate ($Li_{4/3}Ti_{5/3}O_4 + Li^+ + e^- \leftrightarrow Li_{7/3}Ti_{5/3}O_4$, theoretical capacity: 175 mAh g^{-1}) [1]. The electrode potential of $Li_{4/3}Ti_{5/3}O_4$ is 1.5 V relative to Li/Li^+, being higher than that of lithium-intercalated graphite. However, $Li_{4/3}Ti_{5/3}O_4$ is a good candidate as anode material for lithium ion battery with high rate charge/discharge. Therefore many attempts have been made for the preparation of $Li_{4/3}Ti_{5/3}O_4$ with good charge/discharge performance [2–39]. Nano-sized $Li_{4/3}Ti_{5/3}O_4$ powders having large surface areas showed high capacities and good cyclability at high current densities [2–10]. It was shown that fine $Li_{4/3}Ti_{5/3}O_4$ particles with large surface area were needed to keep good electric contact with $Li_{4/3}Ti_{5/3}O_4$. High-density spherical $Li_{4/3}Ti_{5/3}O_4$ powders showed high reversible capacities and cyclability [11,12]. Porous $Li_{4/3}Ti_{5/3}O_4$ [13], nanotube/nanowire of $Li_{4/3}Ti_{5/3}O_4$ [14], $Li_{4/3}Ti_{5/3}O_4$ with hollow-sphere structure [15] and flower-like $Li_{4/3}Ti_{5/3}O_4$ [16] exhibited good electrochemical characteristics. Microwave synthesis gave $Li_{4/3}Ti_{5/3}O_4$ powders with uniform particle size [17]. Composite electrodes such as titanium nitride-coated $Li_{4/3}Ti_{5/3}O_4$ [18], $Li_{4/3}Ti_{5/3}O_4$/carbon nanotube composite [19] and $Li_{4/3}Ti_{5/3}O_4$/polyacene composite [20] were prepared to increase electric contact of insulating $Li_{4/3}Ti_{5/3}O_4$, improving the cycle performance of $Li_{4/3}Ti_{5/3}O_4$ at high current densities. The $Li_{4/3}Ti_{5/3}O_4$ synthesized via a composite molten salt method showed high capacity and good rate performance [21]. Lithium ion cell composed of $Li_{4/3}Ti_{5/3}O_4$ and $LiVPO_4F$ showed good cyclability [22]. It was reported that substitution of a metal such as Mg, Al, Ga or Co for Ti in $Li_{4/3}Ti_{5/3}O_4$ was a good method to increase reversible capacity and to improve cyclability [23,24]. Li-doping into $Li_{4/3}Ti_{5/3}O_4$ increased the capacity and improved cycle performance [25,26]. Br-doping into $Li_{4/3}Ti_{5/3}O_4$ also increased the capacities at high current densities [27]. Thermal properties of $Li_{4/3}Ti_{5/3}O_4$ were investigated by calorimetry [28,29]. Safety problem of $Li_{4/3}Ti_{5/3}O_4$/$LiMn_2O_4$ cell was studied by differential scanning calorimetry (DSC) and accelerated rate calorimetry (ARC). The electrochemical cell showed no thermal runaway, explosion or fire [30]. Safety performance of $Li_{4/3}Ti_{5/3}O_4$ and graphite was also compared using ARC [31]. Substituted lithium titanates of $Li_{4-x}Mg_xTi_{5-x}O_{12}$ ($0 \le x \le 1$) exhibited a high initial discharge capacity of 198 mAh g^{-1} [32]. The $Li_{4/3}Ti_{5/3}O_4$ prepared by spray pyrolysis yielded spherical particles with narrow size distribution [33,34]. Spinel $Li_{4/3}Ti_{5/3}O_4$ prepared by a modified rheological phase method using lithium acetate dehydrate and tetra-n-butyl titanate exhibited high discharge capacities at high current densities [35]. The $Li_{4/3}Ti_{5/3}O_4$ hollow microspheres

* Corresponding author. Tel.: +81 565 488121; fax: +81 565 480076.
E-mail address: nakajima-san@aitech.ac.jp (T. Nakajima).

0378-7753/$ – see front matter © 2010 Elsevier B.V. All rights reserved.
doi:10.1016/j.jpowsour.2010.04.082

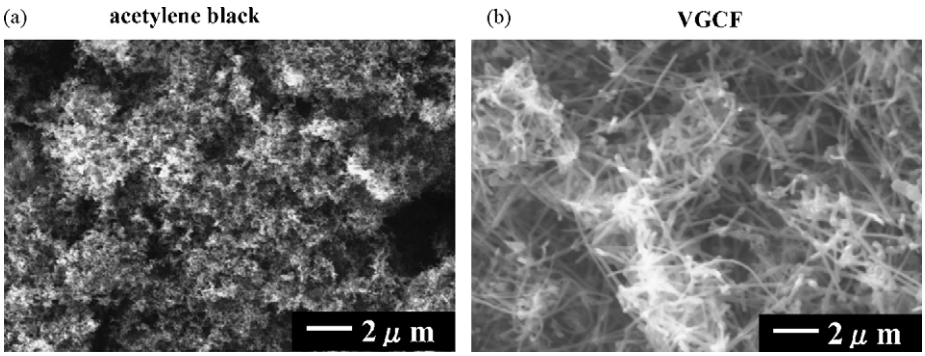

Fig. 1. SEM images of acetylene black (AB) and vapor grown carbon fiber (VGCF).

with nanosheet shell were synthesized by hydrothermal method and calcination kept high discharge capacities even at high current densities [36]. Spinel $Li_4Ti_{5-x}V_xO_{12}$ ($0 \le x \le 0.3$) prepared by solid-state method showed good cycling performance [37]. Nanoscale $Li_4Ti_{5-x}V_xO_{12}$ synthesized by pyrolysis of an aerosol precursor also showed high capacities [38].

A conductive additive giving electric contact between $Li_{4/3}Ti_{5/3}O_4$ particles and current collector plays an important role for the utilization of insulating electrode materials. Acetylene black (AB) with a large surface area is normally used as a conductive additive. It was reported in the previous papers that vapor grown carbon fiber (VGCF) used as a conductive additive and surface fluorination of $Li_{4/3}Ti_{5/3}O_4$ by F_2 increased the charge capacities of $Li_{4/3}Ti_{5/3}O_4$ and thermal stability of electrolyte solution, respectively [39,40]. VGCF is prepared by CVD using Fe catalyst, consisting of thin carbon fibers with diameters of 40–100 nm. VGCF with fibrous structure would have improved the electric contact of $Li_{4/3}Ti_{5/3}O_4$ with a nickel current collector. Uniform mixing of VGCF with $Li_{4/3}Ti_{5/3}O_4$ particles had a difficulty because thin carbon fibers were twined with each other in the case of VGCF. In the present study, mixtures of VGCF and AB were used to obtain the better electric contact between $Li_{4/3}Ti_{5/3}O_4$ particles (average particle size: 4.6 μm) and nickel current collector. Surface modification of $Li_{4/3}Ti_{5/3}O_4$ was performed by using NF_3 and ClF_3 to improve the electrode characteristics of $Li_{4/3}Ti_{5/3}O_4$. The effect of VGCF as a conductive additive on the charge/discharge behavior of surface-fluorinated $Li_{4/3}Ti_{5/3}O_4$ was also investigated.

2. Experimental

2.1. Conductive additives and surface fluorination of $Li_{4/3}Ti_{5/3}O_4$

Fig. 1 shows acetylene black (AB) (BET surface area: 67.6 $m^2\,g^{-1}$) and vapor grown carbon fiber (VGCF) heat-treated at 2800 °C (BET surface area: 11.3 $m^2\,g^{-1}$) used as conductive additives in the study. Lithium titanate, $Li_{4/3}Ti_{5/3}O_4$ (purity: >99.98%, average particle size: 4.6 μm, BET surface area: 2.8 $m^2\,g^{-1}$) supplied by KCM Corporation was used in the present study. Fig. 2 shows a SEM image of original $Li_{4/3}Ti_{5/3}O_4$ sample. The SEM image indicates that $Li_{4/3}Ti_{5/3}O_4$ consists of coagulated particles with a diameter of ca. 1 μm. Particle size distribution data gave two peaks at 2.3 and 17.4 μm. Therefore the average particle size is 4.6 μm and BET surface area is 2.8 $m^2\,g^{-1}$ as described above. Surface fluorination of $Li_{4/3}Ti_{5/3}O_4$ was made by NF_3 gas (5×10^4 Pa) at 100, 150 and 200 °C for 3 min and ClF_3 gas (5×10^4 Pa) at 70, 100 and 200 °C for 3 min. The $Li_{4/3}Ti_{5/3}O_4$ sample (300 mg) put in a nickel boat was placed in a nickel reactor and then fluorinated using NF_3 and ClF_3 gases under the above conditions. Surface structure and composition were analyzed by X-ray diffractometry (Shimadzu, XRD-610), X-ray photoelectron spectroscopy (XPS) (Kratos, ESCA-3400) and BET surface area measurement using nitrogen gas (Shimadzu, Tristar 3000).

2.2. Electrochemical measurements

The $Li_{4/3}Ti_{5/3}O_4$ and AB, VGCF or their mixture were dispersed in N-methyl-2-pyrrolidone (NMP) containing 12 wt% polyvinylidene-fluoride (PVdF). The slurry was pasted on a foamed nickel sheet. The prepared electrode was dried at 120 °C for 12 h in vacuum oven and then pressed before use. The mixing ratio of $Li_{4/3}Ti_{5/3}O_4$:AB, VGCF or VGCF + AB:PVdF was 6:2:2 by weight. The mixing ratios of VGCF + AB mixtures were 1:1 and 1:2 by weight. A three-electrode cell with $Li_{4/3}Ti_{5/3}O_4$ working electrode and Li counter and reference electrodes was used for galvanostatic charge/discharge experiments. The electrolyte solution was 1 mol l^{-1} $LiClO_4$—EC/DEC (1:1 vol.). Charge/discharge cycling was performed at current densities of 60, 300 and 600 mA g^{-1} between 1.0 and 3.0 V vs Li/Li^+ in a glove box filled with Ar at 25 °C.

3. Results and discussion

3.1. Effect of conductive additives on the charge/discharge characteristics of original $Li_{4/3}Ti_{5/3}O_4$

Fig. 3 shows charge/discharge potential curves at 1st cycle and charge capacities and coulombic efficiencies for original $Li_{4/3}Ti_{5/3}O_4$ as a function of cycle number at current densi-

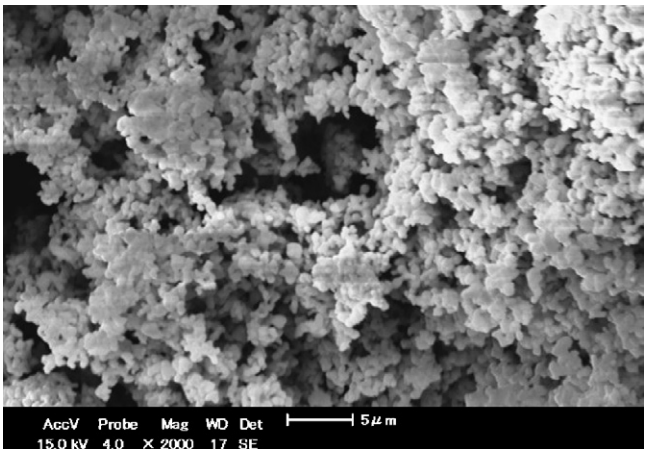

Fig. 2. SEM image of original $Li_{4/3}Ti_{5/3}O_4$ sample.

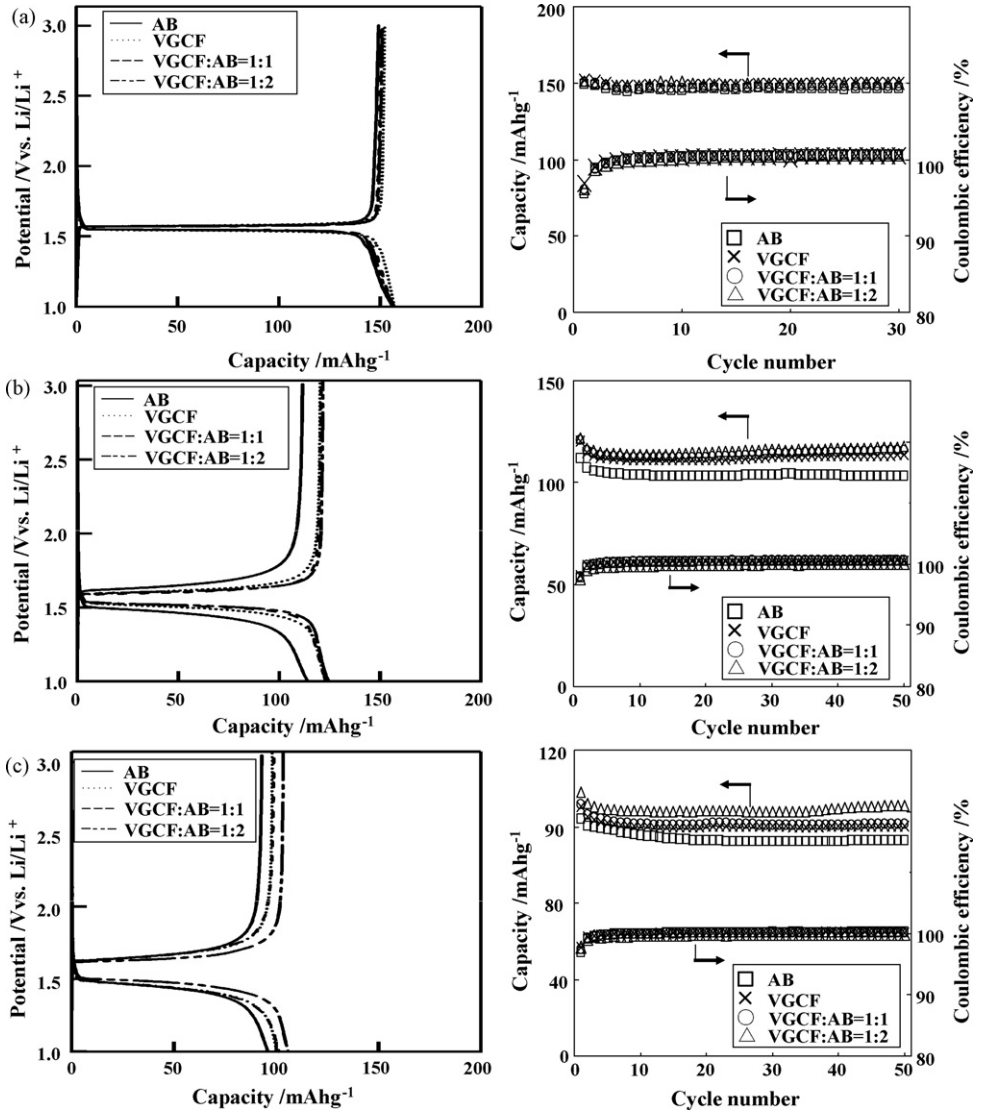

Fig. 3. First charge/discharge potential curves, and charge capacities and columbic efficiencies for original $Li_{4/3}Ti_{5/3}O_4$ as a function of cycle number, obtained at current densities of (a) 60 mA g^{-1}, (b) 300 mA g^{-1} and (c) 600 mA g^{-1} in 1 mol l^{-1} $LiClO_4$—EC/DEC (1:1 vol.). $Li_{4/3}Ti_{5/3}O_4$:(AB, VGCF or VGCF + AB):PVdF = 6:2:2 by weight. —, □: AB, ···, ×: VGCF, - - -, ◯: VGCF:AB = 1:1 by weight, — ·· — ·· —, △: VGCF:AB = 1:2 by weight.

ties of 60, 300 and 600 mA/g. The charge/discharge capacities and coulombic efficiencies were nearly the same at 60 mA g^{-1} for all conductive additives. First charge capacities and first coulombic efficiencies were 149–152 mAh g^{-1} and 95.6–96.9%, respectively. Difference in the charge/discharge data was found at high current densities of 300 and 600 mA g^{-1} as shown in Fig. 3. First charge capacities obtained for VGCF, VGCF + AB(1:1) and VGCF + AB(1:2) were 120, 121 and 122 mAh g^{-1}, respectively while that for AB was 112 mAh g^{-1} at 300 mA g^{-1}. First coulombic efficiencies were nearly the same for all conductive additives (97.7–98.1%). At 600 mA g^{-1}, first charge capacities were 93, 98, 99 and 103 mAh g^{-1} for AB, VGCF, VGCF + AB(1:1) and VGCF + AB(1:2). First coulombic efficiencies were also similar to each other (96.9–97.8%). Charge capacities increased in the order, AB < VGCF < VGCF + AB(1:1) < VGCF + AB(1:2) at 300 and 600 mA g^{-1} as shown in Fig. 3. Potential polarization was also smaller when VGCF and the mixtures of VGCF and AB were used as conductive additives. Thus VGCF and VGCF + AB mixtures gave the higher charge capacities for $Li_{4/3}Ti_{5/3}O_4$ (≈4.6 μm) than AB usually used as a conductive additive. The result shows that VGCF with fibrous structure improves the electric contact between $Li_{4/3}Ti_{5/3}O_4$ particles and nickel current collector.

3.2. Effect of surface fluorination on the charge/discharge behavior of $Li_{4/3}Ti_{5/3}O_4$

Surface fluorination was performed using NF_3 and ClF_3 to modify the surface structure of $Li_{4/3}Ti_{5/3}O_4$. SEM images were the same before and after surface fluorination. Fig. 4 shows X-ray diffraction patterns of $Li_{4/3}Ti_{5/3}O_4$ samples fluorinated by NF_3 and ClF_3. No X-ray diffraction lines indicating fluoride and/or oxide fluoride were found in the samples fluorinated by NF_3 while very weak diffraction lines corresponding to Li_2TiF_6 and $TiOF_2$ were detected in those fluorinated by ClF_3. It is known that NF_3 is easily dissociated into F and NF_2 at ca. 200 °C. Therefore the fluorination using NF_3 is a radical reaction. On the other hand, there is a dissociation equilibrium in the case of ClF_3 at high temperatures: $ClF_3 \leftrightarrow F_2 + ClF$. Fluorine substitution for $Li_{4/3}Ti_{5/3}O_4$ was more easily caused by ClF_3 than NF_3. The result indicates that NF_3 is the better fluorinating agent for the surface modification than ClF_3 because no X-ray diffraction lines except those corresponding to $Li_{4/3}Ti_{5/3}O_4$ was detected for the samples fluorinated by NF_3.

Change in surface composition is somewhat different depending on the fluorinating agents as given in Table 1. Surface concentrations of Li and F increased with increasing fluorination temperature

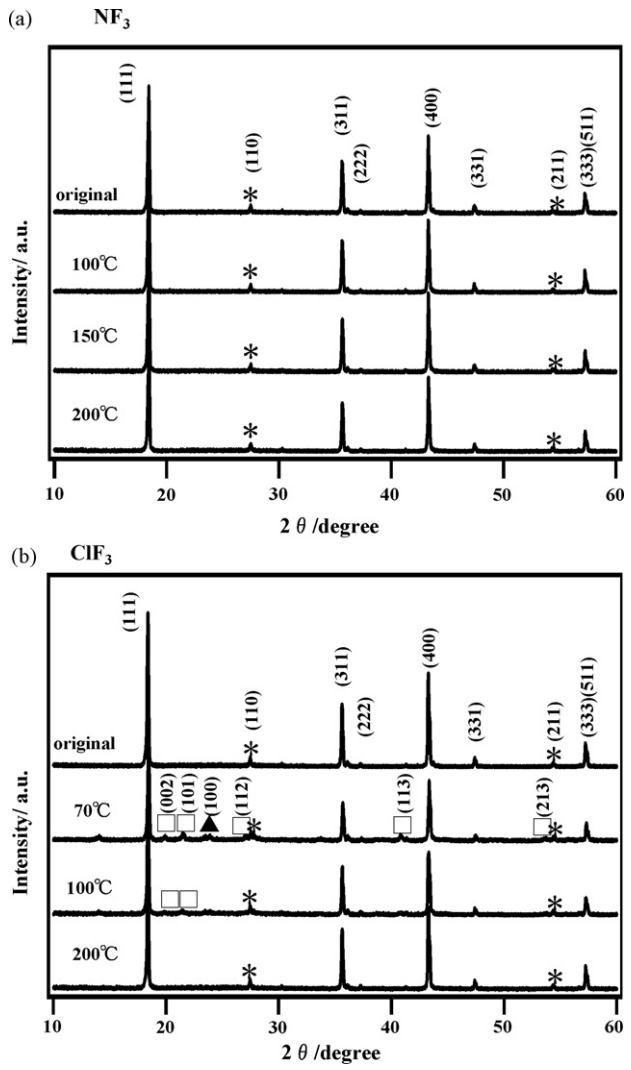

Fig. 4. X-ray diffraction patterns of $Li_{4/3}Ti_{5/3}O_4$ samples fluorinated by (a) NF_3 and (b) ClF_3. *: rutile TiO_2; □: Li_2TiF_6; ▲: $TiOF_2$.

Table 1
Surface composition of $Li_{4/3}Ti_{5/3}O_4$ samples fluorinated by (a) NF_3 and (b) ClF_3.

(a) NF_3					
Fluorination temperature	Surface composition (at.%)				
	Li	Ti	O	F	N
Original	24.6	15.2	60.2	–	–
100 °C	33.4	12.6	44.2	9.8	ND
150 °C	49.0	5.4	20.9	24.7	ND
200 °C	52.7	3.7	15.3	28.3	ND
(b) ClF_3					
Fluorination temperature	Surface composition (at.%)				
	Li	Ti	O	F	Cl
Original	24.6	15.2	60.2	–	–
70 °C	50.5	2.8	14.7	31.9	ND
100 °C	53.4	1.1	9.0	36.5	ND
200 °C	52.0	1.4	10.7	35.9	ND

ND: not detected.

Table 2
First charge/discharge capacities and first coulombic efficiencies for $Li_{4/3}Ti_{5/3}O_4$ fluorinated by NF_3 at (a) 60 mA g^{-1}, (b) 300 mA g^{-1} and (c) 600 mA g^{-1} in 1 mol l^{-1} $LiClO_4$—EC/DEC (1:1 vol.) ($Li_{4/3}Ti_{5/3}O_4$:AB:PVdF = 6:2:2 by weight).

Fluorination temperature	Discharge capacity	Charge capacity	Coulombic efficiency
	(mAh g^{-1})	(mAh g^{-1})	(%)
(a) 60 mA g^{-1}			
Original	156	149	95.6
100 °C	157	149	94.9
150 °C	162	154	95.4
200 °C	153	140	91.4
(b) 300 mA g^{-1}			
Original	114	112	97.7
100 °C	119	115	97.0
150 °C	136	129	95.3
200 °C	118	108	91.0
(c) 600 mA g^{-1}			
Original	96	93	96.9
100 °C	92	88	95.2
150 °C	116	109	94.1
200 °C	87	72	82.3

while those of Ti and O decreased for the samples fluorinated by both NF_3 and ClF_3, which suggests the loss of Ti and O as gaseous O_2, OF_2 and/or TiF_4 and formation of fluoride and oxide fluoride films consisting of LiF, Li_2TiF_6 and/or $TiOF_2$. N and Cl were not detected in all fluorinated samples as given in Table 1. The degree of fluorination was higher in the case of ClF_3. When $Li_{4/3}Ti_{5/3}O_4$ was fluorinated by NF_3 at 100 °C, surface fluorine concentration was relatively low compared with other cases because of the low reactivity of NF_3.

Effect of fluorination on the surface structure was examined by surface area and meso-pore size distribution measurements. BET surface area of original $Li_{4/3}Ti_{5/3}O_4$ was 2.8 m^2 g^{-1}, which increased to 3.4 m^2 g^{-1} by the fluorination with NF_3 at 100 °C, then decreasing to 2.8 and 2.5 m^2 g^{-1} with increasing fluorination temperatures to 150 and 200 °C, respectively. Meso-pore size distribution was significantly changed by surface fluorination. Meso-pores with diameter of 2 nm were largely increased by the fluorination using NF_3 at 100 and 150 °C. Change in the surface area was nearly the same for $Li_{4/3}Ti_{5/3}O_4$ samples fluorinated by ClF_3. The surface areas were 3.0, 2.5 and 2.5 m^2 g^{-1} for the samples fluorinated by ClF_3 at 70, 100 and 200 °C, respectively. Meso-pores with diameter of 2 nm highly increased for the sample fluorinated at 200 °C. The main effect of fluorination on the surface structure of $Li_{4/3}Ti_{5/3}O_4$ was increase in the small meso-pore with diameter of 2 nm.

Fig. 5 shows charge/discharge potential curves and charge capacities and coulombic efficiencies for surface-fluorinated $Li_{4/3}Ti_{5/3}O_4$ samples as a function of cycle number, obtained at a current density of 60 mA g^{-1}. The samples fluorinated by NF_3 at 100 and 150 °C had nearly the same charge/discharge capacities and coulombic efficiencies as those for original $Li_{4/3}Ti_{5/3}O_4$ though the sample fluorinated at 200 °C gave slightly lower values. On the other hand, the samples fluorinated by ClF_3 showed much lower capacities and first coulombic efficiencies than those fluorinated by NF_3. This would be because insulating fluoride and oxide fluoride such as Li_2TiF_6, LiF and/or $TiOF_2$ were formed at the surface. Table 2 shows charge/discharge capacities and coulombic efficiencies at 1st cycle, obtained for $Li_{4/3}Ti_{5/3}O_4$ samples fluorinated by NF_3 at 60, 300 and 600 mA g^{-1} using AB as a conductive additive. First charge capacities for $Li_{4/3}Ti_{5/3}O_4$ samples fluorinated by NF_3 were nearly the same as those for original sample at 60 mA g^{-1}. However, first charge capacities of $Li_{4/3}Ti_{5/3}O_4$ fluorinated at 150 °C increased at the higher current densities of 300 and 600 mA g^{-1}. On the other hand, first charge capacities for

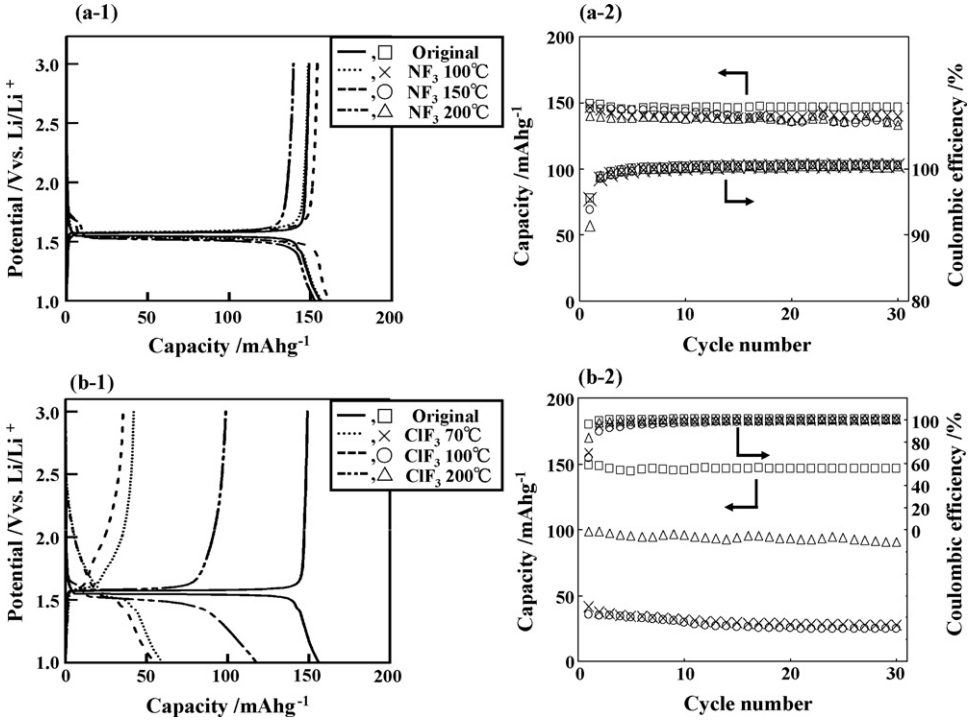

Fig. 5. Charge/discharge potential curves at 1st cycle ((a-1) and (b-1)), and charge capacities and coulombic efficiencies for original and surface-fluorinated $Li_{4/3}Ti_{5/3}O_4$ samples as a function of cycle number ((a-2) and (b-2)). (a-1) and (a-2): —, □: original $Li_{4/3}Ti_{5/3}O_4$, ···, ×: fluorinated by NF_3 at 100 °C, - - -, ○: fluorinated by NF_3 at 150 °C, —··—··—, △: fluorinated by NF_3 at 200 °C. (b-1) and (b-2): —, □: original $Li_{4/3}Ti_{5/3}O_4$, ···, ×: fluorinated by ClF_3 at 70 °C, - - -, ○: fluorinated by ClF_3 at 100 °C, —··—··—, △: fluorinated by ClF_3 at 200 °C.

$Li_{4/3}Ti_{5/3}O_4$ samples fluorinated by ClF_3 were much lower than those for original $Li_{4/3}Ti_{5/3}O_4$. The charge capacities and coulombic efficiencies at 1st cycle were 36–99, 22–64 and 14–34 mAh g^{-1}, and 65–84, 61–81 and 53–70% at current densities of 60, 300 and 600 mA g^{-1}, respectively. Effect of conductive additive was examined for $Li_{4/3}Ti_{5/3}O_4$ samples fluorinated by NF_3, using a mixture of VGCF and AB (1:2 by weight) as a conductive additive. The charge/discharge capacities and coulombic efficiencies at 1st cycle were summarized in Table 3, which shows that $Li_{4/3}Ti_{5/3}O_4$ samples fluorinated at 100 and 150 °C gave the larger first charge capacities than those for original $Li_{4/3}Ti_{5/3}O_4$ and the data shown in Table 2, particularly at high current densities of 300 and 600 mA g^{-1}. The increase in first charge capacities may be due to increase in BET surface area and meso-pore with diameter of 2 nm by surface fluorination.

Table 3
First charge/discharge capacities and first coulombic efficiencies for $Li_{4/3}Ti_{5/3}O_4$ fluorinated by NF_3 at (a) 60 mA g^{-1}, (b) 300 mA g^{-1} and (c) 600 mA g^{-1} in 1 mol l^{-1} $LiClO_4$—EC/DEC (1:1 vol.) ($Li_{4/3}Ti_{5/3}O_4$:VGCF + AB:PVdF = 6:(2/3 + 4/3):2 by weight).

Fluorination temperature	Discharge capacity (mAh g^{-1})	Charge capacity (mAh g^{-1})	Coulombic efficiency (%)
(a) 60 mA g^{-1}			
Original	157	151	96.2
100 °C	162	156	96.1
150 °C	163	155	95.2
200 °C	156	140	89.3
(b) 300 mA g^{-1}			
Original	125	122	97.6
100 °C	155	148	95.5
150 °C	148	143	96.5
200 °C	131	115	88.0
(c) 600 mA g^{-1}			
Original	106	103	97.7
100 °C	133	129	96.8
150 °C	135	123	94.1
200 °C	119	104	87.4

4. Conclusions

Influence of conductive additives and surface fluorination on the charge/discharge characteristics of $Li_{4/3}Ti_{5/3}O_4$ (≈4.6 μm) was investigated using AB and VGCF. VGCF with fibrous structure and mixtures of VGCF and AB (1:1 and 1:2 by weight) increased the charge capacities of original $Li_{4/3}Ti_{5/3}O_4$ and those fluorinated with NF_3 particularly at high current densities of 300 and 600 mA g^{-1} by improving electric contact between $Li_{4/3}Ti_{5/3}O_4$ particles and nickel current collector. Surface fluorination increased meso-pore with diameter of 2 nm and surface area of $Li_{4/3}Ti_{5/3}O_4$, which led to the increase in first charge capacities of $Li_{4/3}Ti_{5/3}O_4$ samples fluorinated by NF_3 at high current densities of 300 and 600 mA g^{-1} for both AB and VGCF + AB mixture as conductive additives. The result shows that NF_3 is better than ClF_3 for surface modification because NF_3 was a mild fluorinating agent for $Li_{4/3}Ti_{5/3}O_4$ between 100 and 200 °C while ClF_3 highly fluorinated $Li_{4/3}Ti_{5/3}O_4$ surface.

Acknowledgement

The authors gratefully thank KCM Corporation for their supplying lithium titanate sample used in the study.

References

[1] T. Ohzuku, A. Ueda, N. Yamamoto, J. Electrochem. Soc. 142 (1995) 1431.
[2] L. Kavan, J. Procházka, T.M. Spitler, M. Kalbáč, M. Zukalová, M. Grätzel, J. Electrochem. Soc. 150 (2003) A1000.
[3] K. Nakahara, R. Nakajima, T. Matsushima, H. Majima, J. Power Sources 117 (2003) 131.
[4] M. Venkateswarlu, C.H. Chen, J.S. Do, C.W. Lin, T.C. Chou, B.J. Hwang, J. Power Sources 146 (2005) 204.
[5] L. Cheng, H.-J. Liu, J.-J. Zhang, H.-M. Xiong, Y.Y. Xia, J. Electrochem. Soc. 153 (2006) A1472.

[6] Y.-J. Hao, Q.-Y. Lai, J.-Z. Lu, H.-L. Wang, Y.-D. Chen, X.-Y. Ji, J. Power Sources 158 (2006) 1358.
[7] J.L. Allen, T.R. Jow, J. Wolfenstine, J. Power Sources 159 (2006) 1340.
[8] J. Li, Y.-L. Jin, X.-G. Zhang, H. Yang, Solid State Ionics 178 (2007) 1590.
[9] C. Jiang, M. Ichihara, I. Honma, H. Zhou, Electrochim. Acta 52 (2007) 6470.
[10] C. Jiang, E. Hosono, M. Ichihara, I. Honma, H. Zhou, J. Electrochem. Soc. 155 (2008) A553.
[11] J. Gao, C. Jiang, J. Ying, C. Wan, J. Power Sources 155 (2006) 364.
[12] J. Gao, J. Ying, C. Jiang, C. Wan, J. Power Sources 166 (2007) 255.
[13] K.-C. Hsiao, S.-C. Liao, J.-M. Chen, Electrochim. Acta 53 (2008) 7242.
[14] J. Li, Z. Tang, Z. Zhang, Electrochem. Commun. 7 (2005) 894.
[15] C. Jiang, Y. Zhou, I. Honma, T. Kudo, H. Zhou, J. Power Sources 166 (2007) 514.
[16] Y.F. Tang, L. Yang, Z. Qiu, J.S. Huang, Electrochem. Commun. 10 (2008) 1513.
[17] L.H. Yang, C. Dong, J. Guo, J. Power Sources 175 (2008) 575.
[18] M.Q. Snyder, S.A. Trebukhova, B. Ravdel, M.C. Wheeler, J. DiCarlo, C.P. Tripp, W.J. DeSisto, J. Power Sources 165 (2007) 379.
[19] J. Huang, Z. Jiang, Electrochim. Acta 53 (2008) 7756.
[20] H. Yu, X. Zhang, A.F. Jalbout, X. Yan, X. Pan, H. Xie, R. Wang, Electrochim. Acta 53 (2008) 4200.
[21] Y. Bai, F. Wang, F. Wu, C. Wu, L.-Y. Bao, Electrochim. Acta 54 (2008) 322.
[22] J. Barker, R.K.B. Gover, P. Burns, A.J. Bryan, Electrochem. Solid-State Lett. 10 (2007) A130.
[23] S. Huang, Z. Wen, Z. Gu, X. Zhu, Electrochim. Acta 50 (2005) 4057.
[24] S. Huang, Z. Wen, X. Zhu, Z. Lin, J. Power Sources 165 (2007) 408.
[25] T. Tabuchi, H. Yasuda, M. Yamachi, J. Power Sources 162 (2006) 813.
[26] H.G. e, N. Li, D. Li, C. Dai, D. Wang, Electrochem. Commun. 10 (2008) 1031.
[27] Y. Qi, Y. Huang, D. Jia, S.-J. Bao, Z.P. Guo, Electrochim. Acta 54 (2009) 4772.
[28] W. Lu, I. Belharouak, J. Liu, K. Amine, J. Power Sources 174 (2007) 673.
[29] W. Lu, I. Belharouak, J. Liu, K. Amine, J. Elecrochem. Soc. 154 (2007) A114.
[30] I. Belharouak, Y.-K. Sun, W. Lu, K. Amine, J. Electrochem. Soc. 154 (2007) A1083.
[31] X.L. Yao, S. Xie, C.H. Chen, Q.S. Wang, J.H. Sun, Y.L. Li, S.X. Lu, Electrochim. Acta 50 (2005) 4076.
[32] A.Y. Shenouda, K.R. Murali, J. Power Sources 176 (2008) 332.
[33] T. Doi, Y. Iriyama, T. Abe, Z. Ogumi, Chem. Mater. 17 (2005) 1580.
[34] S.H. Ju, Y.C. Kang, J. Power Sources 189 (2009) 185.
[35] S.Y. Yin, L. Song, X.Y. Wang, M.F. Zhang, K.L. Zhang, Y.X. Zhang, Electrochim. Acta 54 (2009) 5629.
[36] Y. Tang, L. Yang, S. Fang, Z. Qiu, Electrochim. Acta 54 (2009) 6244.
[37] T.F. Yi, J. Shu, Y.R. Zhu, X.D. Zhu, C.B. Yue, A.N. Zhou, R.S. Zhu, Electrochim. Acta 54 (2009) 7464.
[38] A. Jaiswal, C.R. Horne, O. Chang, W. Zhang, W. Kong, E. Wang, T. Chern, M.M. Doeff, J. Electrochem. Soc. 156 (2009) A1041.
[39] T. Nakajima, A. Ueno, T. Achiha, Y. Ohzawa, M. Endo, J. Fluorine Chem. 130 (2009) 810.
[40] X. Kang, H. Utsunomiya, T. Achiha, Y. Ohzawa, T. Nakajima, Z. Mazej, B. Žemva, M. Endo, J. Electrochem. Soc. 157 (2010) A437.